A Study of Connectivity in MIMO Fading Ad-Hoc Networks

H. Yousefi'zadeh, *Senior Member*, *IEEE*, H. Jafarkhani, *Fellow*, *IEEE*, and J. Kazemitabar

Abstract: **We investigate the connectivity of fading wireless ad-hoc networks with a pair of novel connectivity metrics. Our first metric looks at the problem of connectivity relying on the outage capacity of MIMO channels. Our second metric relies on a probabilistic treatment of the symbol error rates for such channels. We relate both capacity and symbol error rates to the characteristics of the underlying communication system such as antenna configuration, modulation, coding, and signal strength measured in terms of signal-to-interference-noise-ratio. For each metric of connectivity, we also provide a simplified treatment in the case of ergodic fading channels. In each case, we assume a pair of nodes are connected if their bi-directional measure of connectivity is better than a given threshold. Our analysis relies on the central limit theorem to approximate the distribution of the combined undesired signal affecting each link of an ad-hoc network as Gaussian. Supported by our simulation results, our analysis shows that (1) a measure of connectivity purely based on signal strength is not capable of accurately capturing the connectivity phenomenon, and (2) employing multiple antenna mobile nodes improves the connectivity of fading ad-hoc networks.**

Index Terms: **Ad-hoc networks, capacity, central limit theorem, connectivity, multiple-input multiple-output (MIMO) fading channel, random graphs, symbol error rate (SER).**

I. INTRODUCTION

Investigating the connectivity of radio networks goes back to four decades ago. In his pioneering work of [1], Gilbert studied the connectivity of infinite random networks relying on the so-called geometric disk model. In the geometric disk model, a random topology network is represented by a disk graph in which two nodes are directly connected if their distance is smaller than a given transmission radius. As evidenced by the works of [2]–[4], the connectivity of infinite random ad-hoc networks by means of the geometric disk model has recently received much attention. In addition, a survey of the literature reveals a large number of articles in the context of connectivity of ad-hoc networks with a finite number of mobile nodes. Some of the related articles in this area are [5]–[8]. Interestingly, connectivity in random networks represented by graphs of mixed short and long edges can also be related to small world networks [9]. Although originally attractive for studying connectivity, the disk model measures connectivity relying on a pure distance-based metric which is far from the reality of wireless networks. The main disadvantages of the disk model are not considering the effects of fading, attenuation, interference, noise, and mobility.

In [10], signal-to-interference-noise-ratio (SINR) is proposed as the metric of connectivity in wireless ad-hoc networks. According to SINR metric, two nodes in a random topology are connected if their minimum SINR is greater than a given threshold. The two connectivity studies of [11] and [12] rely on the SINR model. While SINR is a more realistic metric of connectivity compared to the geometric disk model, it still falls short of fully capturing the connectivity phenomenon in wireless ad-hoc networks. In reality, a pair of nodes in an ad-hoc network are connected if a sequence of transmitted symbols from one can be received at another. In addition, variations of the channel in time and frequency can also affect connectivity. Utilizing capacity (C) and/or symbol error rate (SER) can better describe the connectivity phenomenon because those quantities are functions of not only fading, shadowing, and power but modulation and antenna configuration.

The use of space-time coding techniques in wireless networks is of special interest because it can substantially reduce the effects of multipath fading in the wireless channels through antenna diversity. Transmit antenna diversity in the form of space-time block codes (STBCs) of [13] and [14] has been adopted in WCDMA and CDMA2000 standards. Receive antenna diversity schemes such as maximum ratio combining (MRC) are already in widespread use in communication systems.

The contributions of our work are in the following areas. We introduce a pair of probabilistic connectivity metrics for wireless ad-hoc networks relying on an analysis of the time-varying fading wireless channels. We utilize central limit theorem and Gaussian approximation in our analysis to represent the combined interference and noise signal affecting the links of an ad-hoc network. Our first metric is defined based on the capacity of multiple-input multiple-output (MIMO) channels. Our second metric is defined based on the symbol error rate of such channels. We also provide a special treatment of our connectivity metrics for ergodic channels. The rest of this paper is organized as follows. Section II, of information theoretic nature, investigates connectivity based on probabilistic and ergodic concepts of capacity in MIMO channels. Section III, also of information theoretic nature, includes a treatment of connectivity based on probabilistic and ergodic measures of SER in such channels. Section IV attempts at capturing the effects of time correlation in the ergodic measures of the previous two sections. In Section V, we numerically validate our connectivity analysis relying on random geometric graph theoretic concepts. Finally, Section VI concludes this paper.

Manuscript received August 03, 2007; approved for publication by Il-Min Kim, Division II Editor, April 08, 2008.

This work was supported in part by the U. S. Army Research Office under the Multi-University Research Initiative (MURI) grant number W911NF-04-1-0224. Preliminary parts of this work appear in the proceedings of IEEE GLOBECOM [20] and IEEE MILCOM [28].

The authors are with the Department of EECS at the University of California, Irvine; email:{hyousefi, hamidj, skazemit}@uci.edu.

II. THE CAPACITY METRIC

The discussion of this section revolves around defining a pair of probabilistic and deterministic metrics of connectivity based on the capacity of wireless MIMO channels. While our general probabilistic metric is defined based on an outage capacity analysis for such channels, our ergodic metric provides a simplified deterministic treatment of the probabilistic metric.

A. Probabilistic Capacity Metric

In this subsection, we introduce our first probabilistic metric of connectivity relying on the concepts of outage capacity and outage probability. Calculating estimates or upper bounds of capacity in the case of uncorrelated and correlated single-input single-output (SISO) and MIMO channels both with Gaussian and non-Gaussian noise has been the subject of heavy research in the past years. The concept of outage capacity was first introduced in [15]. Outage capacity provides an elegant description of the achievable rate of a communication channel. Simply put, it represents a probabilistic measure of the maximum number of bits per cycle that can be transmitted for a given error rate. The authors of [15] also provided approximations of the capacity of identically and independently distributed (i.i.d.) MIMO Rayleigh channels. In [16], methods of calculating the capacity of correlated MIMO channels with Gaussian noise were proposed. The authors of [17] numerically verified that the approximations of capacity derived in [15] work well under various fading conditions in the presence of Rayleigh distributed interference, for a wide signal-to-noise ratio (SNR) range, and even when the channel is semi-temporally correlated.

Our discussion below represents a treatment of the subject material relying on the cited literature articles above. In order to be consistent with the literature work of capacity for MIMO channels, the analysis is carried out by explicitly working with the input and output signals of a fading channel.

Consider an ad-hoc topology with q wireless flat fading links $\{\mathcal{L}_1, \cdots, \mathcal{L}_q\}$ on which transmission powers are $\{P_1, \cdots, P_q\}$, respectively. Link i is associated with the i-th transmitter/receiver pair. Each link may be connecting multiple antenna mobile nodes. Suppose, per symbol transmission power P_i is equally distributed among M_i transmit antennas of link i. The number of receive antennas for link i is assumed to be N_i. Further, let us assume that the matrix H_{ij} represents the fading channel between the transmitter of link j and the receiver of link i. Denoting $\mathbf{S}_i$ as the $M_i \times T$ symbol matrix of link i transmitted over T discrete time blocks, the received symbol matrix at link i is the following $N_i \times T$ matrix

$$\mathbf{R}_i = H_{ii}\mathbf{S}_i + \mathbf{\Gamma}_i \tag{1}$$

where the channel matrices H_{ii} consist of complex Gaussian random variable elements and $\mathbf{\Gamma}_i = \sum_{j \neq i} H_{ij}\mathbf{S}_j + \mathbf{n}_i$ represents the combined effects of interference and noise. We assume that the receiver of link i knows the channel matrix H_{ii} while the transmitter of link i only knows its distribution. The quantities $(\mathbf{\Gamma}_i | H_{ij})$ can be considered to form a Gaussian random process due to the following lines of reasoning. As discussed in Chapter 2 of [18], we know that the codewords $\mathbf{S}_j$ should be chosen from a Gaussian distribution to be capacity achieving. Further, H_{ij}'s are known at the receiver. Since the elements $H_{ij}\mathbf{S}_j$ are linear combinations of independent Gaussian random variables, they are themselves Gaussian. In addition, any $\mathbf{S}_j$ or $\mathbf{n}_i$ term at any given time slot is independent of its counterparts at other time slots. Since the transmitter does not know the channel, it assigns the codewords independently at each time slot. Therefore, $(\mathbf{\Gamma}_i | H_{ij})$ forms a Gaussian random process. The covariance matrix for the resulting noise term is expressed as

$$\begin{aligned} K_i &= E\{\mathbf{\Gamma}_i {\mathbf{\Gamma}_i}^\dagger\} \\ &= E\{(\sum_{j \neq i} H_{ij}\mathbf{S}_j + \mathbf{n}_i)(\sum_{k \neq i} H_{ik}\mathbf{S}_k + \mathbf{n}_i)^\dagger\} \\ &= E\{\sum_{j \neq i} H_{ij}\, \mathbf{S}_j \mathbf{S}_j^\dagger\, H_{ij}^\dagger\} + \overline{P}_i^{(n)}\, I \end{aligned} \tag{2}$$

where the superscript † indicates the Hermitian operator, E represents the expectation operator, and $\overline{P}_i^{(n)}$ is the average power of noise. Since we are assuming that H_{ij} coefficients are known at the receiver,

$$\begin{aligned} K_i &= \sum_{j \neq i} H_{ij}\, E\{\mathbf{S}_j \mathbf{S}_j^\dagger\}\, H_{ij}^\dagger + \overline{P}_i^{(n)}\, I \\ &= \sum_{j \neq i} H_{ij} \Phi_j H_{ij}^\dagger + \overline{P}_i^{(n)}\, I \end{aligned} \tag{3}$$

where I is the identity matrix and Φ_j indicates the covariance matrix of the input signal vector of link j. Then, the mutual information $\mathcal{I}$ between $\mathbf{S}_i$ and $\mathbf{R}_i$ is derived as[1]

$$\mathcal{I}(\mathbf{S}_i; \mathbf{R}_i) = \log_2 \det(I + K_i^{-1} H_{ii} \Phi_i H_{ii}^\dagger). \tag{4}$$

To find the capacity, one needs to maximize $\mathcal{I}(\mathbf{S}_i; \mathbf{R}_i)$ subject to a transmission power constraint $Tr(\Phi_i) \leq P_i$ on link i where $Tr(\Phi_i)$ and P_i denote the trace of Φ_i and the transmission power of link i, respectively.

The choice of covariance matrix achieving the capacity in (4) depends on the realization of the channel matrix. When the channel is not known at the transmitter, the best strategy is to distribute the input power equally among the transmit antennas. The latter results in a covariance matrix Φ_i that is a multiple of the identity matrix. Considering the constraint $Tr(\Phi_i) \leq P_i$, we have $\Phi_i = \frac{P_i}{M_i} I$ resulting in the following capacity determination

$$C_i = \log_2 \det \left(I + \frac{P_i}{M_i} K_i^{-1} H_{ii} H_{ii}^\dagger \right) \quad \text{bps/Hz}. \tag{5}$$

Note that the capacity can be expressed in terms of a natural logarithm rather than a base 2 logarithm assuming the unit of measurement is changed from bps/Hz to nats/sec/Hz.

In the most general case, the capacity expression of (5) can be only calculated numerically. When the number of links is relatively large, one can utilize central limit theorem to conclude that the covariance matrix of (3) can be expressed as a multiple of the identity matrix. The reasoning is follows. Relying on the equation $\Phi_i = \frac{P_i}{M_i} I$, we note that the first term of the covariance matrix K_i is in the form of $\sum_{j \neq i} \frac{P_j}{M_j} H_{ij} H_{ij}^\dagger$. Since the

[1]The symbol $\mathcal{I}$ used to denote mutual information should be distinguished from the symbol I to denote the identity matrix.

non-diagonal entries of the first term are the sum of zero-mean random variables, central limit theorem implies that they tend to the mean value of the random variables, zero. Further, the diagonal entries of the first term consist of the sum of the square of the magnitudes of the channel coefficients from interfering links. Consequently, they represent the power of interfering signals. Thus, the covariance matrix of (3) is expressed in the following form

$$K_i \simeq [\overline{P}_i^{(I)} + \overline{P}_i^{(n)}]\, I \tag{6}$$

where $\overline{P}_i^{(I)}$ and $\overline{P}_i^{(n)}$ are the average power of interference and noise, respectively. Therefore, (5) can be rewritten as follows

$$C_i \simeq \log_2 \det\left(I + \frac{\overline{SINR}_i}{M_i} H_{ii} H_{ii}^{\dagger}\right) \quad \text{bps/Hz} \tag{7}$$

with $\overline{SINR}_i$ denoting the average SINR. Next, we note that the capacity in (7) is defined for a fixed realization of the fading channel H_{ii} at link i over a large block length. Every realization of the channel has some probability attached to it through the statistical model of H_{ii}. We assume that the matrix H_{ii} consists of zero-mean Gaussian random variables, i.e., each element of the matrix has a fading envelope described by Rayleigh distribution. It is well known [19] that the sum of q zero-mean i.i.d. complex Gaussian random variables with a standard deviation $1/\sqrt{2\lambda}$ is a zero-mean Gaussian random variable with a standard deviation $\sqrt{q/2\lambda}$. Since the channel matrices H_{ii} are random in nature, the capacity in (7) can be treated as a random variable.

According to singular value decomposition (SVD) theorem, C_i can be calculated in terms of the positive eigenvalues of $H_{ii}H_{ii}^{\dagger}$ as

$$C_i \simeq \sum_{l=1}^{\rho} \log_2\left[1 + \frac{\overline{SINR}_i}{M_i}\sigma_l\right] \quad \text{bps/Hz} \tag{8}$$

where σ_l, $l \in \{1, \cdots, \rho\}$ denote the positive eigenvalues of $H_{ii}H_{ii}^{\dagger}$ and ρ is the rank of H_{ii}. Therefore, the capacity C_i represents a scalar function of the set of random variables $\{\sigma_1, \cdots, \sigma_\rho\}$. Our work of [20] describes how the probability density function (pdf) of capacity can be calculated depending on the values of M_i and N_i. Here, we summarize the results. The PDF of $H_{ii}\, H_{ii}^{\dagger}$ for the case of $M_i \times N_i = 1 \times 1$ is described in the form of

$$f_z(z) = \lambda\, e^{-\lambda z}. \tag{9}$$

The pdf identified above represents the only positive eigenvalue of the scalar function $H_{ii}\, H_{ii}^{\dagger}$. For the cases of $M_i \times N_i = 2 \times 1$ and $M_i \times N_i = 1 \times 2$, the pdf of $H_{ii}\, H_{ii}^{\dagger}$ is expressed as

$$f_z(z) = \lambda^2 z e^{-\lambda^2 z}. \tag{10}$$

Again, the pdf identified above represents the only positive eigenvalue of $H_{ii}\, H_{ii}^{\dagger}$. The results for the case of $M_i \times N_i = 2 \times 2$ are numerically calculated similar to the case of $M_i \times N_i = 2 \times 1$ with an H_{ii} matrix consisting of four pairs of complex Gaussian random variables.

Treating capacity as a random variable with a given pdf provides us with an opportunity to represent a novel connectivity metric based on the concept of outage capacity. We introduce our first metric of connectivity as

$$Pr(C_i < C_{out}) \leq \Delta_C \tag{11}$$

where $Pr(\cdot)$, C_{out}, and Δ_C represent probability, the threshold of connectivity also known as outage capacity, and the outage probability, respectively. While our definition of outage matches that of [15], it differs slightly from that of [16]. According to [16], the outage is defined as

$$\inf_{Tr(\Phi_i) \leq P_i} Pr(C_i < C_{out}) \leq \Delta_C. \tag{12}$$

The main difference between the two definitions is that the latter may assign zero power to some of the transmit antennas while the former utilizes all of the antennas. According to our outage capacity metric matching the former definition, two nodes are connected if the probability of the outage event for the link between them is less than a given value.

B. Deterministic Capacity Metric

In this subsection, we provide a deterministic treatment of the connectivity metric of the previous subsection assuming the underlying wireless channel is ergodic. The ergodic capacity $\overline{C}_i$ of link i can be expressed as [16]

$$\begin{aligned} \overline{C}_i &= E\,[\,C_i\,] \\ &\simeq E\left[\log_2 \det\left(I + \tfrac{\overline{SINR}_i}{M_i} H_{ii} H_{ii}^{\dagger}\right)\right] \quad \text{bps/Hz.} \end{aligned} \tag{13}$$

Utilizing SVD theorem and the results of random matrix theory, the following expression can be derived for the ergodic capacity of MIMO channels.

$$\overline{C}_i \simeq u \int_0^{\infty} \log_2\left(1 + \frac{\overline{SINR}_i}{M_i} x\right) f_x(x)\, dx. \tag{14}$$

In (14), $f_x(\cdot)$ represents the pdf of a randomly selected eigenvalue of the Wishart matrix defined as

$$f_x(x) = \frac{1}{u}\sum_{k=0}^{u-1} \frac{k!\, x^{v-u}\, e^{-x}}{(k+v-u)!}\left[\Lambda_k^{v-u}(x)\right]^2, \quad x \geq 0 \tag{15}$$

with parameters $u = \min(M_i, N_i)$ and $v = \max(M_i, N_i)$. In (15), $\Lambda_k^m(x)$ denotes the Laguerre polynomial of order k defined as

$$\begin{aligned} \Lambda_k^m(x) &= \tfrac{e^x\, x^{-m}}{k!}\tfrac{d^k}{dx^k}\{e^{-x}\, x^{k+m}\} \\ &= \sum_{h=0}^{k} (-1)^h \binom{k+m}{k+h} \frac{x^h}{h!} \end{aligned} \tag{16}$$

where $\binom{k+m}{k+h}$ is the binomial coefficient.

In [21], a simplified expression for the ergodic capacity of (14) is derived under average transmit power and equal power allocation constraints as

$$\begin{aligned} \overline{C}_i \simeq\ & e^{\frac{M_i}{\overline{SINR}_i}} \log_2 e \\ & \times \textstyle\sum_{k=0}^{u-1} \sum_{l=0}^{k} \sum_{m=0}^{2l} \left[\frac{(-1)^m (2l)!(v-u+m)!}{2^{2k-m}\, l!\, m!\, (v-u+l)!}\right. \\ & \left. \times \binom{2k-2l}{k-l}\binom{2l+2v-2u}{2l-m} \sum_{n=0}^{v-u+m} \Psi_{n+1}\left(\tfrac{M_i}{\overline{SINR}_i}\right)\right] \end{aligned} \tag{17}$$

where $\Psi_n(z)$ is defined as

$$\Psi_n(z) = \int_1^\infty e^{-zx}\, x^{-n}\, dx, \quad n = 0, 1, \cdots \tag{18}$$

with $Re(z) > 0$.

Using the ergodic capacity of (13) or equivalently (17), we can introduce a more simplified connectivity metric in the form of

$$\overline{C}_i \geq C_{out} \tag{19}$$

where C_{out} is the threshold of connectivity.

III. THE SER METRIC

The discussion of this section revolves around providing probabilistic and deterministic measures of connectivity based on SER. SER can in turn be related to the characteristics of the underlying communication system such as SINR, modulation, and antenna configuration.

A. Probabilistic SER Metric

Once again, consider the ad-hoc topology described previously consisting of q flat fading wireless links $\{\mathcal{L}_1, \cdots, \mathcal{L}_q\}$ on which transmission powers are $\{P_1, \cdots, P_q\}$, respectively. Associated with each element $H_{ij}(n,m)$ of channel matrices, we define the fading factors $F_{ij}(n,m) = |H_{ij}(n,m)|^2$. For each link i, the SER can be derived as an exact function of the average SINR and the corresponding fading factors $F_{ii}(n,m)$.

We start by investigating the expressions of SER for $1 \times N_i$ link i. In [22], the expressions of SER for $1 \times N_i$ link i in terms of the number of signal points in the constellation and the average SNR can be found. The calculations of [22] are carried out under the assumption of facing a complex Gaussian noise signal. As one of the operating scenarios, the calculations are carried out for a Rayleigh fading channel and utilizing PSK modulation. Because the quantity of interest is SINR rather than SNR in the context of current discussion, we need to investigate the effects of interference signals in (1). First, we claim that the product $H_{ij}\mathbf{S}_j$ remains Gaussian in (1). Using a limited constellation set like BPSK with a uniform distribution for each signal instead of capacity achieving codebook, we verify the claimed statement for the case of 1×1 link. Generalization to L-PSK modulation and $M_i \times N_i$ link is then straightforward. If we use BPSK modulation, $H_{ij}\mathbf{S}_j$ will be a scalar random variable with the following description

$$\mathbf{X}_j = H_{ij}\mathbf{S}_j = \begin{cases} H_{ij}, & \text{with probability } 0.5 \\ -H_{ij}, & \text{with probability } 0.5. \end{cases} \tag{20}$$

To see why $\mathbf{X}_j$ is a complex Gaussian random variable, we need to show that both real and imaginary parts of this random variable are normally and independently distributed. Since

$$\begin{aligned} Re\{\mathbf{X}_j\} &= Re\{H_{ij}\mathbf{S}_j\} \\ &= \begin{cases} Re\{H_{ij}\}, & \text{with probability } 0.5 \\ -Re\{H_{ij}\}, & \text{with probability } 0.5, \end{cases} \end{aligned} \tag{21}$$

we have

$$\begin{aligned} & Pr(Re\{\mathbf{X}_j\} < x) \\ &= \tfrac{1}{2} Pr(Re\{H_{ij}\} < x) + \tfrac{1}{2} Pr(-Re\{H_{ij}\} < x) \\ &= Pr(Re\{H_{ij}\} < x). \end{aligned} \tag{22}$$

Therefore, the distribution of the real part of $\mathbf{X}_j$ is normal. Relying on the same argument, the distribution of the imaginary part of $\mathbf{X}_j$ is normal. Next, we observe

$$\begin{aligned} & Pr(Re\{X_j\} < x \mid Im\{X_j\} < y) \\ =\ & Pr(Re\{X_j\} < x \mid Im\{X_j\} < y,\, S_j = 1) Pr(S_j = 1) \\ & + Pr(S_j Re\{X_j\} < x \mid Im\{X_j\} < y,\, S_j = -1) Pr(S_j = -1) \\ =\ & \tfrac{1}{2} Pr(Re\{X_j\} < x \mid Im\{X_j\} < y,\, S_j = -1) \\ & + \tfrac{1}{2} Pr(-Re\{X_j\} < x \mid -Im\{X_j\} < y,\, S_j = -1) \\ =\ & \tfrac{1}{2} Pr(Re\{X_j\} < x) + \tfrac{1}{2} P(-Re\{X_j\} < x) \\ =\ & Pr(Re\{X_j\} < x) \end{aligned} \tag{23}$$

which concludes our reasoning of independence.

Since the product $H_{ij}\mathbf{S}_j$ remains Gaussian in (1) and the sum of Gaussian random variables is still Gaussian [19], the signal $\mathbf{\Gamma}_i$ can still be treated as Gaussian. However, the resulting Gaussian noise is now colored rather than being white. We note that applying maximum likelihood (ML) decoding as utilized by [22] to a colored Gaussian noise results in sub-optimality, i.e., identifying upper bounds of the SER. Based on the argument above, the analysis of [22] can still be applied to the case of SINR utilizing the model of (1) the same way it is applied to SNR.

According to Section 9.2 of [22], the expressions of SER are calculated for a $1 \times N_i$ link i utilizing MRC and BPSK modulation as

$$SER_i \simeq Q\left(\sqrt{2 \sum_{n=1}^{N_i} F_{ii}(n,1)\, \overline{SINR}_i}\right) \tag{24}$$

where $\overline{SINR}_i$ is the average received SINR and the Gaussian Q function is defined as

$$\begin{aligned} Q(x) &= \frac{1}{\sqrt{2\pi}} \int_x^\infty \exp\left(-\frac{z^2}{2}\right) dz \\ &= \frac{1}{\pi} \int_0^{\pi/2} \exp\left(-\frac{x^2}{2\sin^2\phi}\right) d\phi \end{aligned} \tag{25}$$

Relying on the discussion of Section 4.9 of [18], we note that the MRC expressions of (24) can also be applied to Alamouti STBCs of [14] with proper scaling factors. Particularly, the results of a 1×2 link utilizing MRC codes can be applied to the case of a 2×1 link utilizing Alamouti codes. Similarly, the results of a 1×4 link utilizing MRC codes can be applied to the case of a 2×2 link utilizing Alamouti codes.

Utilizing BPSK modulation and under the assumption of facing a Rayleigh fading channel, the symbol error rate of link i can be derived from the latter analysis as

$$SER_i \simeq Q\left(\sqrt{2\,\eta\,\Upsilon_i\, \overline{SINR}_i}\right) \tag{26}$$

where $\overline{SINR}_i$ is the average SINR of link i and η is a constant that depends on the antenna configuration. While the value of η is 1 for 1×1 and 1×2 links utilizing MRC, it changes to 0.5

for 2×1 and 2×2 links utilizing STBCs of [13]. Further, Υ_i is defined as

$$\Upsilon_i = \sum_{m=1}^{M_i} \sum_{n=1}^{N_i} F_{ii}(n,m). \tag{27}$$

Since the quantity SER_i as specified by (26) represents a function of random variables, it suffices to examine the distribution of $F_{ii}(n,m)$ in order to obtain fading statistics of SER_i. We start from the case of a single transmit and single receive antenna link, i.e., $F_{ii} = F_{ii}(1,1)$ and $M_i = N_i = 1$. In a 1×1 link case and when the channel matrix is identified by a complex Gaussian noise element, one can conclude that $r_i = |H_{ii}|$ has a marginal Rayleigh density function [19] in the form of

$$p_r(r_i) = \frac{r_i e^{-r_i^2/2\mu_i^2}}{\mu_i^2}, \quad r_i \geq 0 \tag{28}$$

where μ_i^2 equals to half of the average power of all of the multipath components. The pdf of F_{ii} can be expressed [19] as

$$p_F(F_{ii}) = \frac{1}{2\sqrt{F_{ii}}} p_r(\sqrt{F_{ii}}). \tag{29}$$

Once the pdfs of F_{ii} terms are calculated and assuming they are spatially uncorrelated, the pdf of Υ_i is specified [19] as defined in (27). Finally, the pdf of SER_i as defined in (26) can be numerically calculated in terms of the pdfs of random variables Υ_i.

Having captured the distribution of the SER for a MIMO link, we are now ready to express our second metric of connectivity in terms of the quantities of interest. We introduce our second metric of connectivity as

$$Pr(SER_i > S_{out}) \leq \Delta_S \tag{30}$$

where $Pr(.)$, S_{out}, and Δ_S represent probability, the threshold of connectivity, and the outage probability, respectively.

B. Deterministic SER Metric

In this subsection, we assume that the time-varying fading wireless channel is ergodic. Under the assumption of facing an ergodic Rayleigh channel and utilizing BPSK modulation, the random variable SER_i of (26) can be substituted by its average value $\overline{SER_i}$ defined as

$$\overline{SER_i} \simeq \int_0^\infty \frac{1}{\pi} \int_0^{\pi/2} \exp\left(-\frac{2\,\eta\,\Upsilon_i\,\overline{SINR_i}}{2\sin^2\tau}\right) d\tau p_\Upsilon(\Upsilon_i) d\Upsilon_i \tag{31}$$

where $p_\Upsilon(.)$ is the PDF of the random variable Υ_i. The result is also valid for L-PSK modulation as

$$\overline{SER_i} \simeq \int_0^\infty \frac{1}{\pi} \int_0^{\frac{(L-1)\pi}{L}} \exp\left(-\frac{2\eta\Upsilon_i\overline{SINR_i}}{2\sin^2\tau}\right) d\tau p_\Upsilon(\Upsilon_i) d\Upsilon_i. \tag{32}$$

In [23], closed-form expressions of the integral of (32) are calculated. The expressions describe the SER of a MIMO channel in terms of the number of signal points in the constellation and the average SNR. We carry out our calculations under the assumption of facing a slow fading ergodic Rayleigh channel and utilizing the PSK modulation scheme. In what follows, we provide the results of our calculations considering the fact that in the current discussion the quantity of interest is $\overline{SINR}$ rather than $\overline{SNR}$. First, we introduce the SER of a $1 \times N_i$ link i using MRC as

$$\begin{aligned}\overline{SER_i} \simeq\ & \tfrac{L_i-1}{L_i} \\ & -\tfrac{1}{\pi}\sqrt{\tfrac{\vartheta_i}{1+\vartheta_i}}\Big\{(\tfrac{\pi}{2}+\tan^{-1}\theta_i)\textstyle\sum_{j=0}^{N_i-1}\binom{2j}{j}\frac{1}{[4(1+\vartheta_i)]^j} \\ & +\sin(\tan^{-1}\theta_i)\textstyle\sum_{j=1}^{N_i-1}\sum_{k=1}^{j}\frac{\zeta_{kj}}{(1+\vartheta_i)^j} \\ & \times[\cos(\tan^{-1}\theta_i)]^{2(j-k)+1}\Big\}\end{aligned} \tag{33}$$

where $\vartheta_i = \overline{SINR_i}\sin^2(\frac{\pi}{L_i})$, $\theta_i = \sqrt{\frac{\vartheta_i}{1+\vartheta_i}}\cot\frac{\pi}{L_i}$, and $\zeta_{kj} = \binom{2j}{j}/\binom{2(j-k)}{j-k}4^i[2(j-k)+1]$.

Noting that the number of bits per symbol is related to the number of signal points in the constellation L_i as $\log_2 L_i$, the result of (33) for a 1×1 link utilizing BPSK modulation with $L_i = 2$ is expressed as

$$\overline{SER_i} \simeq \frac{1}{2}\left(1 - \sqrt{\frac{\overline{SINR_i}}{1+\overline{SINR_i}}}\right). \tag{34}$$

Similarly, the result of (33) for a 1×2 link utilizing BPSK modulation is expressed as

$$\overline{SER_i} \simeq \frac{1}{2}\left[1 - \sqrt{\frac{\overline{SINR_i}}{1+\overline{SINR_i}}}\left(1 + \frac{1}{2(1+\overline{SINR_i})}\right)\right]. \tag{35}$$

We observe that the SER of a 1×2 link is improved compared to that of a 1×1 link due to the receive diversity gain.

Further, we note that the SER of Alamouti STBCs of [13] and [14] can be derived from Section II.A of [23]. Based on that discussion and for a fixed transmit power, one can derive the symbol error rate of a 2×1 link by replacing $\overline{SINR_i}$ with $\frac{\overline{SINR_i}}{2}$ in (35). Similarly, one can obtain the symbol error rate of a 2×2 link by using the results of a 1×4 link. With the choice of BPSK modulation, the result for a 2×2 link is expressed as

$$\overline{SER_i} \simeq \frac{1}{2} - \frac{1}{2}\sqrt{\frac{\overline{SINR_i}}{2+\overline{SINR_i}}}\left(\sum_{j=0}^{3}\binom{2j}{j}\frac{1}{[2(2+\overline{SINR_i})]^j}\right). \tag{36}$$

Using the ergodic SER above, we can introduce a simplified connectivity metric in the form of

$$\overline{SER_i} \leq S_{out} \tag{37}$$

where S_{out} is the threshold of connectivity.

IV. CAPTURING TEMPORAL CORRELATION OF ERGODIC CHANNELS

Up until now, we have assumed that the wireless fading channel is flat implying no temporal correlation exists among the

symbols of a single frame. In this section, we capture the effects of temporal correlation on our connectivity metrics. We propose a scheme in which the temporally correlated fading channel is modeled by a finite-state Markov chain. Our scheme can be applied to the cases of our ergodic connectivity metrics. Capturing temporal correlation in the cases of our probabilistic metrics is more complex and the subject of our future study.

A finite-state Markov chain is a discrete-time representation of the behavior of a random variable. Each state is associated with an average quantity representing the value of the random variable at that state. The chain is fully specified by the set of average per state quantities and a set of per state steady-state probabilities. For an S-state chain, S per state average quantities and S steady-state probabilities can be calculated by partitioning the pdf of a random variable with a set of threshold values $\{\xi_0, \cdots, \xi_S\}$ associated with the observed behavior of the random variable.

While such Markov chain modeling approach can be applied to any number of states, we note that utilizing a larger number of states improves the accuracy of the model at the cost of increasing the complexity of calculations. We propose the use of a two-state chain with two states G and B to address the tradeoff between computational complexity and model accuracy. Utilizing a two-state Markov chain applied to the pdf of C_i in (8), the ergodic connectivity metric of (19) still holds when the ergodic average $\overline{C}_i$ of link i is expressed as

$$\overline{C}_i = \pi_{i,G}^{(C)} \ \overline{C}_{i,G} + \pi_{i,B}^{(C)} \ \overline{C}_{i,B} \tag{38}$$

where $\pi_{i,G}^{(C)}$ and $\pi_{i,B}^{(C)}$ represent per state steady-state probabilities derived from the ratios of surface integrals of the pdf of C_i within appropriate threshold bounds. Further, average per state quantities $\overline{C}_{i,G}$ and $\overline{C}_{i,B}$ are specified as the ratios of expectation integrals and surface integrals of the pdf of C_i within appropriate threshold bounds [24]. Similarly and utilizing a two-state Markov chain applied to the pdf of SER_i in (26), the ergodic connectivity metric of (37) still holds when the ergodic average $\overline{SER}_i$ of link i is expressed as

$$\overline{SER}_i = \pi_{i,G}^{(SER)} \ \overline{SER}_{i,G} + \pi_{i,B}^{(SER)} \ \overline{SER}_{i,B} \tag{39}$$

with similar description of quantities in (38) derived from the pdf of SER_i in (26) instead of those derived from the pdf of C_i in (8).

V. EXPERIMENTAL VERIFICATION OF ANALYSIS

This section is dedicated to the evaluation of effectiveness for the information theoretic metrics of connectivity introduced in previous sections. It consists of two subsections. The objective of the first subsection is to show why utilizing a metric purely based on SINR cannot capture the reality of connectivity in fading ad-hoc networks. The objective of the second subsection is to investigate the results of applying the metrics of previous sections to a random network topology.

A. Justification of Proposed Connectivity Metrics

We open this section by providing a justification of using our proposed metrics of connectivity instead of the SINR metric.

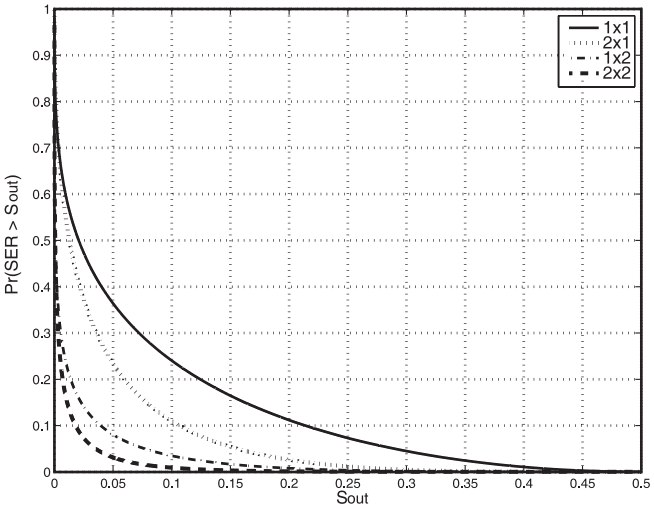

Fig. 1. Normalized BPSK plots of $1 - CDF(SER)$ versus S_{out} for a wireless link utilizing different antenna configurations with $SINR = 3$ dB.

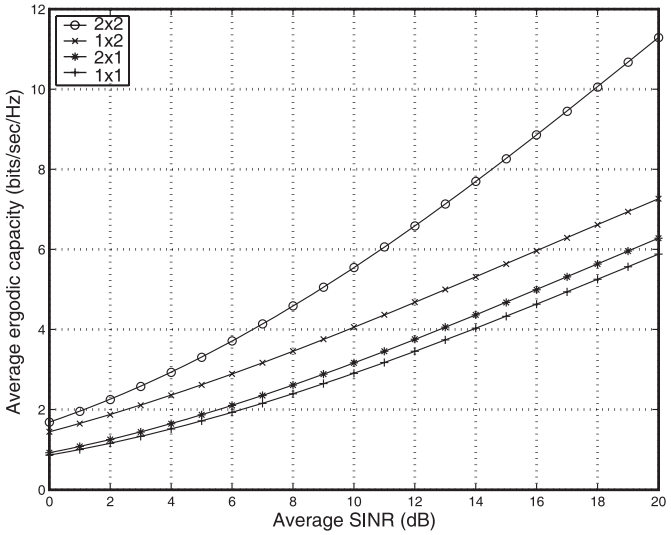

Fig. 2. BPSK plots of $\overline{C}$ versus $\overline{SINR}$ for an isolated wireless link utilizing different antenna configurations.

For different choices of antenna configurations of a given link, Fig. 1 depicts normalized values of $1-CDF(SER)$ versus S_{out} where $CDF(SER)$ indicates the cumulative distribution function (cdf) of SER. For a choice of S_{out} on the horizontal axis of each figure, the corresponding value on the vertical axis represents the value $Pr(SER > S_{out})$. Thus, the connectivity metric may be satisfied if the horizontal line representing Δ_S is located above the value of $Pr(SER > S_{out})$. The figure reveals the fact that the probabilistic measure of the SER can be different for the same threshold S_{out} based on the antenna configuration. For example, for the choice of $(S_{out}, \Delta_S) = (0.15, 0.1)$, the connectivity metric of (30) is satisfied for 2×1, 1×2, and 2×2 antenna configurations but not 1×1 antenna configuration. While not shown here, similar results are observed in the case of outage capacity metric of connectivity.

For an isolated point-to-point transmission scenario and dif-

ferent antenna configurations, Fig. 2 depicts $\overline{C}$ as defined in (17) versus $\overline{SINR}$. We note that in an isolated point-to-point communication scenario, there is no interference term and as a result the term $\overline{SINR}$ is the same as $\overline{SNR}$. The figure reveals that the capacity can be different for the same signal strength based on the antenna configuration. For example for the choice of $\overline{SINR} = 10$ dB and $C_{out} = 5$ bps/Hz in Fig. 2, the connectivity metric of (19) is only satisfied for 2×2 wireless links but not the other antenna configurations.

Hence, depending on the thresholds of connectivity C_{out}, S_{out}, Δ_C, and Δ_S that are determined by the computing platform of a mobile node, a pure measurement of the signal strength such as SINR is not sufficient to capture the connectivity phenomenon.

B. Connectivity Experiments

In this subsection, we apply our proposed connectivity metrics to a moderate size random ad-hoc topology. In order to provide a meaningful basis of comparison, we compare our results for the same random topology. In our random topology, 200 nodes are distributed on a 2-D domain with an area of 1000 square meters according to a Poisson point process [25]. When measuring connectivity, we assume all of the nodes can transmit at the same time. We note that the use of Gaussian approximation according to central limit theorem is justified for different antenna configurations as the result of allowing simultaneous transmissions and considering the number of interfering nodes. More specifically, we have conducted a number of experiments to quantify the number of independent interference terms necessary for accurate use of Gaussian approximation. Our experiments have revealed that the use of Gaussian approximation is acceptable with an accuracy of 0.01% when the number of interference terms, each term contributed by an individual path, exceeds 30. The latter translates to 30 nodes in the case of 1×1 antenna configurations and no more than 8 nodes in the case of 2×2 antenna configurations.

The following describes general settings of our experiments. All of the nodes are assumed to be utilizing BPSK modulation. In our probabilistic experiments, we assume that the slow fading wireless channel characterized by a Rayleigh distribution is quasi-static and flat implying there is no temporal correlation between a pair of symbols belonging to the same frame. In our ergodic experiments, we utilize a two-state Markov chain when partitioning the pdfs of the random variables associated with capacity and SER. In both cases, we set the partitioning thresholds as $\{\xi_0, \xi_1, \xi_2\} = \{0, 1.2039, 10\}$. We assume that each node utilizes a total transmission power of $P = 1\ W$ on the combined set of its outgoing links. In the case of multiple antenna nodes, the total transmission power is split equally among the antenna paths, i.e., M_i signals are transmitted simultaneously from the M_i transmit antennas at each time slot using Alamouti STBCs of [13] and [14]. The expected value of the noise power on each path is assumed to be $10\ \mu W$. Depending on a specific experiment, a pair of nodes are considered to form a direct link if one of the probabilistic connectivity metrics of (11) and (30) or one of the ergodic connectivity metrics of (19) and (37) holds. A direct link is formed only if both of its nodes can transmit and receive from each other under a connectivity criterion.

Table 1. A comparison of the relative sizes of the largest connected cluster utilizing outage capacity connectivity metric.

	$C_{out} = 2$ $\Delta_C = 0.01$	$C_{out} = 1.5$ $\Delta_C = 0.01$	$C_{out} = 1$ $\Delta_C = 0.02$
1×1	1.5%	2%	7%
HYBRID	12.0%	31.0%	90.5%
2×2	90.5%	94.0%	98.0%

Table 2. A comparison of the the relative sizes of the largest connected cluster utilizing ergodic capacity connectivity metric.

	$C_{out} = 3.8$	$C_{out} = 4$
1×1	32.5%	17.5%
HYBRID	85.5%	85.5%
2×2	98.0%	98.0%

Table 3. A comparison of the relative sizes of the largest connected cluster utilizing probabilistic SER connectivity metric.

	$S_{out} = 0.01$ $\Delta_S = 0.01$	$S_{out} = 0.02$ $\Delta_S = 0.01$	$S_{out} = 0.05$ $\Delta_S = 0.02$
1×1	1.5%	1.5%	7%
HYBRID	29.5%	33.0%	87.5%
2×2	68.5%	83.5%	92.5%

Table 4. A comparison of the the relative sizes of the largest connected cluster utilizing ergodic SER connectivity metric.

	$S_{out} = 0.0001$	$S_{out} = 0.01$
1×1	1%	8.0%
HYBRID	4.0%	87.0%
2×2	17.5%	92.5%

For the random topology described above, we consider three scenarios. In the first scenario which serves as our base line SISO scenario, the network is only accommodating single antenna mobile nodes. We refer to this scenario as the 1×1 case. In the second scenario exactly half of the mobile nodes are randomly selected to be equipped with double antennas. We refer to this scenario as the HYBRID case. In the third scenario to which we refer as the 2×2 case, the network is only accommodating double antenna mobile nodes.

We provide the results of our experiments in the case of the probabilistic measures of (11) and (30) as well as ergodic measures of (19) and (37). It is important to note that all of our measures implicitly capture the effects of shadowing and distance in addition to fading. The latter is due to the fact that the measures are all expressed as a function of average SINR. We refer the reader to the work of [24] to see how shadowing, distance, and fading are captured in the calculations of average SINR. For the random topology network above, Fig. 3 includes sample connectivity graphs chosen from among a large set of experiments run with different combinations of simulation parameters. While the parameter settings of the graphs merely represent our sampling choices, the results of all of our experiments remain consistent. We refer the reader to our related work of [26] where we investigate the effects of parameter variations on connectivity.

Reviewing the connectivity graphs, we observe that they vary depending on not only the SINR measure but modulation, antenna configurations, and other settings of the nodes. While a pure measurement of the signal strength such as SINR is not quite capable of describing the phenomenon of connectivity,

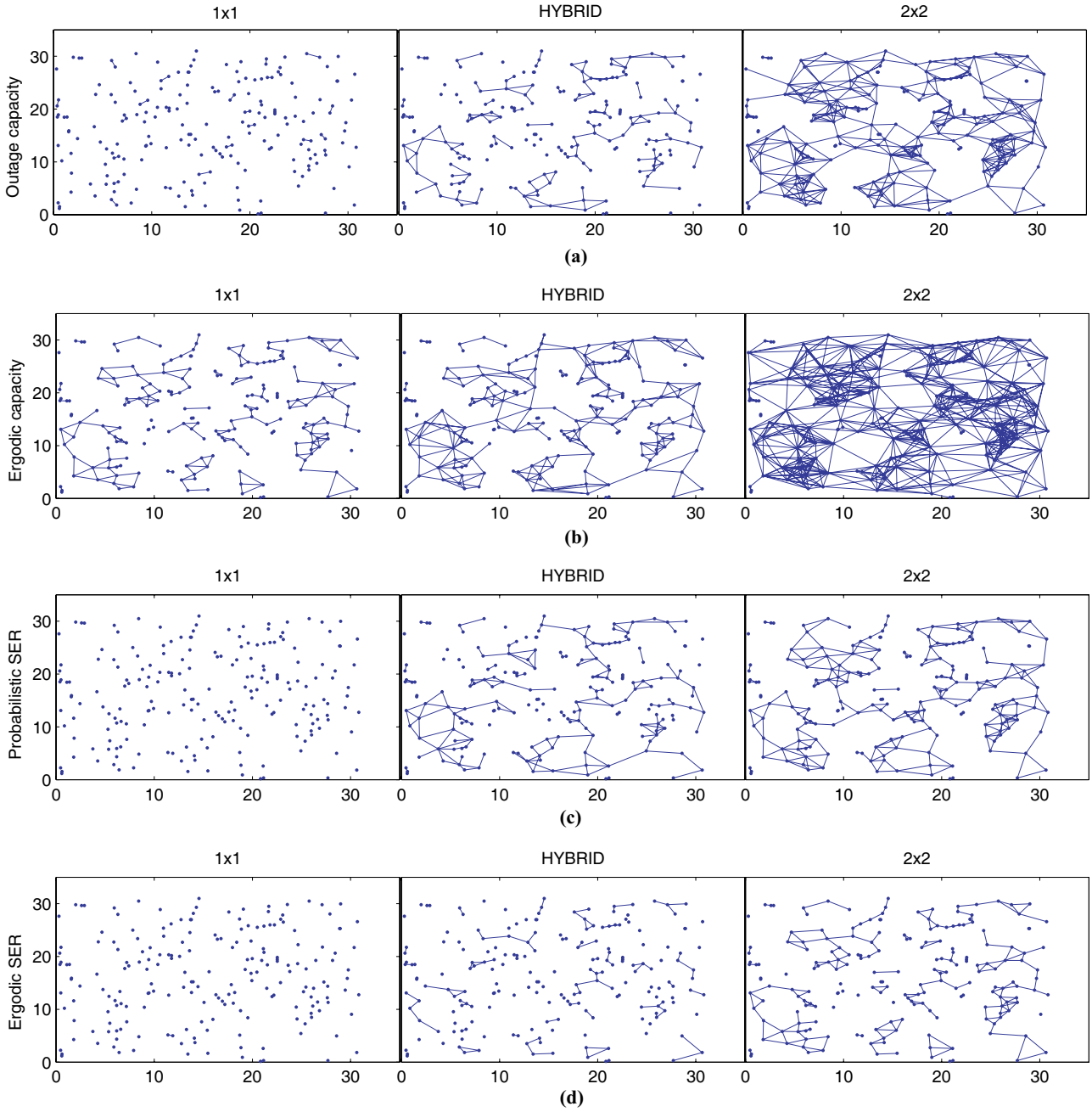

Fig. 3. Connectivity graphs of a random topology network in a square domain of 1000 square meters. The columns from left to right correspond to single antenna, hybrid, and double antenna mobile nodes. (a) The illustrations of the first row show the results of utilizing probabilistic connectivity metric of (11) with $C_{out} = 2$ bps/Hz and $\Delta_C = 0.01$. (b) The illustrations of the second row show the results of utilizing ergodic connectivity metric of (19) with $C_{out} = 4$ bps/Hz. (c) The illustrations of the third row show the results of utilizing probabilistic connectivity metric of (30) with $S_{out} = 0.02$ and $\Delta_S = 0.01$. (d) The illustrations of the fourth row show the results of utilizing ergodic connectivity metric of (37) with $S_{out} = 0.0001$.

utilizing one of our proposed metrics provides a better way of properly capturing the effects of the quantities of interest when investigating connectivity.

From the results of the experiments, we can also calculate the percentages of the nodes belonging to the largest connected cluster of nodes. The larger the percentage, the closer the network to being fully connected and a measure of 100% is associated with a fully connected network. Utilizing the connectivity metrics of (11) and (19), Tables 1 and 2 report the connectivity results for different combination of choices of C_{out} and Δ_C with similar other settings. We observe that decreasing the value of C_{out} and increasing the value of Δ_C increases the size of the largest cluster of the connectivity graph.

Similarly, utilizing the SER connectivity metrics of (30) and (37), Tables 3 and 4 report the results for different combination of choices of S_{out} and Δ_S with similar other settings. We notice that increasing the values of S_{out} and Δ_S increases the size of the largest cluster observed in the connectivity graph.

At the end of this section, it is worth mentioning that the calculation costs of our measures of connectivity, accrued at each

node and particularly under mobility, are relatively higher than those of the distance and SINR measures. Nonetheless, we believe that the increased computational cost of our approach is justified in order to create accurate benchmarks capable of truly capturing the connectivity phenomenon. While this work has proposed analytical measures for studying connectivity, we are currently working on developing intelligent schemes resulting in the reduction of the calculation costs of our measures under mobility. Finally, we would like to point out that the existence of error recovery and scheduling schemes utilized by medium access control (MAC) technologies at the link layer can and will affect connectivity. Capturing the combined effects of PHY and MAC layers is outside the scope of this study and is the subject of future studies.

VI. Conclusion

In this paper, we investigated the connectivity of fading wireless ad-hoc networks. By defining a pair of probabilistic metrics of connectivity, we investigated the problem of connectivity based on the capacity of MIMO channels and their symbol error rate rather than the received signal strength. We also provided simplified measures of connectivity in the case of ergodic MIMO channels. In such cases, we captured the temporal correlation of the channel by utilizing a finite-state Markov chain the parameters of which were obtained by partitioning the pdf of the random variables of interest, $\overline{C}_i$ and $\overline{SER}_i$. Our results clearly showed that the use of signal-to-interference-noise ratios cannot properly capture the connectivity phenomenon in wireless ad-hoc networks. They also showed that the use of multiple antenna mobile nodes improves the connectivity of wireless ad-hoc networks utilizing any of our proposed connectivity metrics. Comparing the two capacity- and SER-based metrics of connectivity discussed in this paper, one may note that the latter metric provides a more practical alternative for use in ad-hoc networks. Our future research is focused on analyzing the effects of small world phenomenon [9] in placement algorithms of advantaged mobile nodes in order to improve the connectivity of wireless ad-hoc networks. In addition, we are investigating the applicability of our connectivity results in the context of scheduling and cross-layer routing schemes for wireless ad-hoc networks.

REFERENCES

[1] E. N. Gilbert, "Random plane networks," *SIAM J.*, vol. 9, pp. 533–543, 1961.

[2] L. Booth, J. Bruck, M. Franschetti, and R. Meester, "Continuum percolation and the geometry of wireless networks," *Ann. Applied Probability*, 2002.

[3] T. K. Philips, S. S. Panwar, and A. N. Tantawi, "Connectivity properties of a packet radio network model," *IEEE Trans. Inf. Theory*, Sept. 1989.

[4] S. Quintanilla, S. Torquato, and R. M. Ziff, "Efficient measurements of the percolation threshold for the fully penetrable disks," *J. Physics*, Oct. 2000.

[5] Y.-C. Cheng and T. G. Robertazzi, "Critical connectivity phenomena in multihop radio models," *IEEE Trans. Commun.*, July 1989.

[6] P. Santi and D. M. Blough, "An evaluation of connectivity in mobile wireless ad hoc networks," in *Proc. IEEE DSN*, 2002.

[7] C. Bettstetter, "On the minimum node degree and connectivity of a wireless multihop network," in *Proc. ACM MOBIHOC*, 2002.

[8] O. Dousse, P. Thiran, and M. Hasler, "Connectivity in ad-hoc and hybrid networks," in *Proc. IEEE INFOCOM*, 2002.

[9] D. Watts and S. Strogatz, "Collective dynamics of small-world networks," *Nature*, June 1998.

[10] P. Gupta and P. R. Kumar, "The capacity of wireless networks," *IEEE Trans. Inf. Theory*, Mar. 2000.

[11] F. Baccelli and B. Blaszczyszyn, "On a coverage process ranging from the boolean model to the poisson Voronoi tessellation, with applications to wireless communications," *AAP*, vol. 33, no. 2, 2001.

[12] O. Dousse, F. Baccelli, and P. Thiran, "Impact of interferences on connectivity in ad-hoc and networks," in *Proc. IEEE INFOCOM*, 2003.

[13] S. M. Alamouti, "A simple transmitter diversity scheme for wireless communications," *IEEE J. Sel. Areas Commun.*, Nov. 1998.

[14] V. Tarokh, H. Jafarkhani, and A. R. Calderbank, "Space-time block coding from orthogonal designs," *IEEE Trans. Inf. Theory*, July 1999.

[15] G. J. Foschini and M. J. Gans, "On limits of wireless communication in a fading environment when using multiple antennas," *Wireless Personal Commun.*, Mar. 1998.

[16] I. E. Telatar, "Capacity of multi-antenna gaussian channels," *European Trans. Telecommun.*, Nov.–Dec. 1999.

[17] M. Kang, M.-S. Alouini, and G. E. Oien, "How accurate are the gaussian and gamma approximations to the outage capacity of MIMO channels?," in *Proc. Baiona Workshop on Signal Processing in Communications*, 2003.

[18] H. Jafarkhani, *Space-Time Coding: Theory and Practice*, Cambridge University Press, 2005.

[19] A. Papoulis and S. U. Pillai, *Probability, Random Variables, and Stochastic Processes, Fourth Edition*, McGraw-Hill, 2002.

[20] H. Jafarkhani, H. Yousefi'zadeh, and J. Kazemitabar, "Capacity-based connectivity of MIMO fading ad-hoc networks," in *Proc. IEEE GLOBECOM*, 2005.

[21] H. Shin and J. H. Lee, "Closed-form formulas for ergodic capacity of MIMO rayleigh fading channels," in *Proc. IEEE ICC*, 2003.

[22] M. K. Simon and M. S. Alouini, *Digital Communication over Fading Channels: A Unified Approach to Performance Analysis*, John Wiley, 2000.

[23] H. Yousefi'zadeh, H. Jafarkhani, and M. Moshfeghi, "Power optimization of wireless media systems with space-time block codes," *IEEE Trans. Image Process.*, July 2004.

[24] L. Zheng, H. Yousefi'zadeh, and H. Jafarkhani, "Resource allocation in fading wireless ad-hoc networks with temporally correlated loss," in *Proc. IEEE WCNC*, 2004.

[25] JFC Kingman, *Poisson Processes*, Oxford University Press, 1993.

[26] J. Kazemitabar, H. Yousefi'zadeh, and H. Jafarkhani, "The impacts of physical layer parameters on the connectivity of ad-hoc networks," in *Proc. IEEE ICC*, 2006.

[27] C. E. Shannon, *The Mathematical Theory of Information*, University of Illinois Press, 1949 (Reprinted 1998).

[28] H. Yousefi'zadeh, H. Jafarkhani, and J. Kazemitabar, "SER-based connectivity of fading ad-hoc networks," in *Proc. IEEE MILCOM*, 2005.

Homayoun Yousefi'zadeh Homayoun Yousefi'zadeh received the B.S. degree from Sharif University of Technology, the M.S. degree from Amirkabir University of Technology, and the Ph.D. degree from University of Southern California all in electrical engineering, in 1989, 1993, and 1997, respectively. He is currently with the faculty of the Department of Electrical Engineering and Computer Science at the University of California, Irvine. He also holds a consulting scientist position at the Boeing company. Most recently, he was the founder and CTO of TierFleet, Inc. working on distributed database systems, a senior technical and business manager at Procom Technology focusing on storage networking, and a technical consultant at NEC Electronics designing and implementing distributed client-server systems. He has served as the founding chairperson of the systems' management workgroup of the Storage Networking Industry Association (SNIA), and a member of the scientific advisory board of the Integrated Media Services Center (IMSC) at the University of Southern of California. He is a recepient of UCI Faculty Award in 2003. He is an Associate Editor for the IEEE COMMUNICATIONS LETTERS, an Editor of the IEEE WIRELESS COMMUNICATIONS, and has been with the TPC of various IEEE conferences. He is a Senior Member of IEEE.

Hamid Jafarkhani Hamid Jafarkhani received the B.S. degree in electronics from Tehran University in 1989 and the M.S. and Ph.D. degrees both in electrical engineering from the University of Maryland at College Park in 1994 and 1997, respectively. In 1997, he was a Senior Technical Staff Member at AT&T Labs-Research and was later promoted to a Principle Technical Staff Member. He is currently a Professor at the Department of Electrical Engineering and Computer Science, University of California, Irvine, where he is also the Deputy Director of Center for Pervasive Communications and Computing. He ranked first in the nationwide entrance examination of Iranian universities in 1984. He was a co-recipient of the American Division Award of the 1995 Texas Instruments DSP Solutions Challenge. He received the Best Paper Award of ISWC in 2002, the 2006 IEEE Marconi Best Paper Award in Wireless Communications, and an NSF Career Award. He also received the UCI Distinguished Mid-Career Faculty Award for Research in 2006 and the School of Engineering Fariborz Maseeh Best Faculty Research Award in 2007. He was an Associate Editor for IEEE Communications Letters from 2001–2005, an Editor for the IEEE Transactions on Wireless Communications from 2002–2007 and an Editor for the IEEE Transactions on Communications from 2005–2007. Currently, he is an Area Editor for the IEEE Transactions on Wireless Communications. He is listed as a highly cited researcher in http://www.isihighlycited.com. He is an IEEE Fellow and the author of the book "Space-Time Coding: Theory and Practice."

Seyed Javad Kazemitabar Seyed Javad Kazemitabar was born in Babol, Iran in March 1981. He received the B.S. degree from Sharif University of Technology, Tehran, Iran in 2003, and M.S. and Ph.D. degree from University of California, Irvine in 2005 and 2008, respectively, all in electrical engineering. His research interests include multiple antenna communications, joint routing, and scheduling for wireless networks. In 1998, he won the silver medal in Iran national Mathematics Olympiad. He also ranked third in the nationwide entrance examination of Iranian universities in 1999. He is currently with Wilinx Corp. in Carlsbad, working on UWB systems.